MALAYSIAN JOURNAL OF MICROSCOPY

Journal homepage: https://malaysianjournalofmicroscopy.org

RESEARCH ARTICLE

EFFECT OF PMMA, PS, AND PEO POLYMERS ON PHYSICAL PROPERTIES OF POLY (O-TOLUIDINE).TiO_2 NANOCOMPOSITE BLEND

Hadi Hassan Mohammed[1], Hadeel Tariq Hamad[2], Hayder Mohammed Ali[3], Tariq J. Alwan[4,*]

[1]Ministry of Education, Directorate-General for Education Dhi Qar, Iraq
[2]Ministry of Education, Directorate of Education of First Karkh, Baghdad, Iraq
[3]Ministry of Education, Directorate of Education of First Al-Rusafa, Baghdad, Iraq
[4]Mustansiriyah University, College of Education, Physics Department, Baghdad, Iraq

Abstract. The films of Poly O-toluidine. Titanium dioxide (POT.TiO_2), mixed with different types of conventional polymers were effectively created via casting method. TiO_2 nanoparticles were used as reinforcement in POT blends (POT.TiO_2/PMMA, POT.TiO_2/PS, and POT.TiO_2/PEO) with constant concentration to improve their mechanical and electrical properties. The POT.TiO_2 nanocomposites were produced using in-situ chemical oxidative polymerizatione. The morphology, structural characteristics, and functional groups of the produced samples were examined using field-emission scanning electron microscopy FE-SEM, X-ray diffraction XRD, and Fourier transform infrared spectroscopy FTIR. FE-SEM images show that the morphology of POT.TiO_2/PMMA and POT.TiO_2/PS films is approximately similar; they appear as semi-spherical and spherical protrusions structures. The situation is different in POT.TiO_2/PEO, as the morphology has rough and disorganized. The characteristic peaks in all the samples indicated a polycrystalline structure of the films, also the XRD spectra, indicated that the addition of conventional polymers enhanced the crystallinity state of POT.TiO_2. Electrical conductivity was assessed using the two-probe method at room temperature and found the POT.TiO_2/PEO film demonstrated the maximum value of electrical conductivity of about 2.81×10^{-8} S.cm^{-1}. The mechanical properties of the prepared samples were determined by measuring their tensile and hardness. The POT.TiO_2/PMMA film had the highest tensile and hardness values. This study looked at what happens when the type of conventional polymer is changed and how that changes the electrical and mechanical properties of POT.TiO_2 blends, with the aim of improving the mechanical and electrical properties for polymer films.

Keywords: Polymer blends films, Poly (O-Toluidine), TiO_2 nanoparticles.

Article Info

Received 11 May 2024
Accepted 11 November 2024
Published 6 December 2024

***Corresponding author: tariq@uomustansiriyah.edu.iq**

ISSN: 1823-7010, eISSN: 2600-7444

1. INTRODUCTION

Conductive polymers have unique properties of a mixture between metals and their electrical properties and the advantages of conventional polymers, with lower cost, lighter weight, and corrosion resistance [1].

One of the conductive polymers that researchers concentrate on is POT. Due to its poor processability and mechanical characteristics, POT has limited applications [2]. The POT can be blended with one or more conventional polymers to improve its mechanical properties, resulting in a novel POT blend with distinct physical features [3].

The most popular conventional polymers used in conductive polymer blends are poly (methyl methacrylate) PMMA, polystyrene PS, and poly (ethylene oxide) PEO. PMMA is obtained by polymerization of methyl methacrylate. It is characterized by its transparency (excellent optical properties, 92% light transmission), its ease of implementation, its mechanical properties (rigidity and impact resistance), its dielectric properties, and its resistance to aging (excellent UV resistance) [4].

Polystyrene, commonly called crystal polystyrene because of its transparency, results from the polymerization of styrene under the action of catalysts. It is characterized by rigidity and brittleness. High-impact polystyrene, a translucent or opaque product, resulting from a copolymerization by grafting with an elastomer, polybutadiene or poly(butadiene/styrene), which gives it reduced rigidity and good impact resistance (3 to 10% butadiene) [5].

Poly (ethylene oxide) is characterized by its solubility in water and ethanol and has a melting point of 54-58 ˚C, while its density ranges from 1.1 -1.2 gm\cm^3, and it is in the form of a white solid with a moderate odor and has excellent solubility and good thermal stability. Radiation, especially UV radiation with a short wavelength and high energy, greatly affects poly (ethylene oxide) due to its ability to dissolve and form free radicals. This leads to the formation of cross-linking, which in turn transforms the polymer from a transparent state to an opaque one due to the formation of crystalline regions. It is also affected by reinforcement with different types of reinforcing materials, such as changes in hardness, strength, and fracture toughness [6].

However, another difficulty arose for researchers, that is, the electrical characteristics of conductive polymers are adversely affected by mixing with conventional polymers, TiO_2 nanoparticles were used as reinforcement in POT blends to enhance their mechanical and electrical properties [7].

A POT.TiO_2 nanocomposite is a POT matrix with TiO_2 nanoparticles; it has unique features that cannot be attained by each component functioning independently. To incorporate TiO_2 nanoparticles into the POT structure, a polymerization process is used in the presence of TiO_2 nanoparticles. Because of the formation of POT.TiO_2 networks, POT.TiO_2 nanocomposites possess distinctive physical and chemical properties that have made them a pioneer in a wide range of electronic applications, especially organic electronics [8].

Using conductive polymers doped with semiconductor oxides and conventional polymers is helpful because it combines the electrical and optical properties of the conductive polymers and semiconductor oxides with the mechanical properties of conventional polymers, such as plasticity. Due to their properties, these blends are particularly interesting in several areas of commercial applications: Organic solar cells, organic light-emitting diodes, organic field-effect transistors, antistatic coatings, rechargeable batteries, electrolytic capacitors, conductive coatings, electromagnetic shielding, chemical or biological sensors [9-10].

The main goal of this study is to synthesize POT.TiO_2 nanocomposites by using site-polymerization and to investigate the effects of blending POT.TiO_2 with different conventional polymers (PMMA, PS, and PEO). The study aims to evaluate and compare the structural, mechanical, and electrical properties of these blends to determine the most effective conventional polymer for

enhancing the performance of POT.TiO_2 in creating polymer composite films with optimized electrical conductivity and mechanical strength. This will provide insights into which polymer blend is most suitable for potential applications in flexible electronics, energy storage, and advanced materials.

2. MATERIALS AND METHODS

2.1 Materials

The following chemical materials are used in the research is shown in Table 1.

Table 1: Employed chemicals materials.

Chemical materials	Mw g/mol
O-Toluidine	107.16
Hydrochloric Acid (HCl)	36.46
TiO_2 nanopartials powder	79.88
Chloroform ($CHCl_3$)	119.20
Ammonium persulphate $(NH4)_2S_2O_8$	228.20
Poly(methyl methacrylate)	35000
Polystyrene	32000
Poly (ethylene oxide)	200000
Distilled water	---

2.2 Preparation of POT.TiO_2

POT.TiO_2 nanocomposites were prepared using in-situ oxidative polymerization, by dissolving 2.5 g O-Toluidine in 1 M HCl and then adding 0.2 g TiO_2 nanoparticles to obtain O-Toluidine.TiO_2 solution. 0.2 g of TiO_2 is the minimum weight added that shows improvement in the properties of POT. A monomer/oxidant was used, similar to the one reported by Jameel et al. [11] and Alwan [12], who obtained the emeraldine salt of POT.TiO_2 powder. A POT.TiO_2 film cannot be prepared by casting method because when the solvent evaporates after casting, the POT.TiO_2 returns to the powder state since it does not dissolve in most solvents but rather spreads in them, and the POT solution does don't have viscosity.

2.3 Preparation of POT.TiO_2/PMMA, POT.TiO_2/PS, POT.TiO_2/PEO Films

Films were created using POT.TiO_2 blends via casting method. First, a POT.TiO_2 solution was produced by dissolving 0.05 g of POT.TiO_2 powder in 5 mL of chloroform. The solution was stirred for 2 hours to ensure homogeneity. Then it was added 0.2 g PMMA to the POT.TiO_2 solution and kept under continuous stirring for another two hours to get the POT.TiO_2/PMMA solution. The procedure was repeated: 0.07 g PEO and 0.2 g PS were added, to prepare POT.TiO_2/PEO and POT.TiO_2/PS solutions, respectively. Weights of 0.2 and 0.07 g of (PMMA, PS) and PEO were chosen because they are the minimum amount from which polymer films can be obtained, in addition, the films are the same thickness. Used a Petri dishes to cast samples from the previously prepared solutions and allowed to dry for four days at room temperature to create the films.

2.4 Thickness Measurement

The thickness of the samples is an important parameter in studying the physical properties of the films. All samples must have the same thickness to facilitate comparisons. The thickness of the samples was measured using a digital micrometer, and it was found that the thickness of the samples is within the limits of 63±10 μm.

2.5 Field-Emission Scanning Electron Microscope (FE-SEM)

A field-emission scanning electron microscope (TESCAN MIRA3 FS-SEM) was used to look at the particles of the samples and see things like their size, shape, and how their sizes were spread out. It is necessary to coat the samples with gold before imaging.

2.5 Fourier Transforms Infrared Spectroscopy (FTIR)

A Fourier transform infrared spectrophotometer (FTIR-8400S) provided by Shimadzu was used to characterize the prepared polymer films. This instrument operates within the range of (500-4000) cm-1. FT-IR measurement is essential for identifying the functional groups in polymer films and is a good method for detecting types of bonds in samples.

2.6 X-Ray Diffraction

This type of examination is carried out to study the crystal structure of the prepared samples. This is achieved by studying the X-ray diffraction pattern of the films, which identifies the locations of the peaks that appear when a beam of X-rays is directed at specific angles on the film's surface. According to Bragg's Law, these peaks are caused by X-ray waves reflecting off of parallel crystal surfaces. These surfaces cause constructive interference for the waves, which is what these peaks are. In the current study, an X-ray diffraction device was used with the following specifications: Type: Philips, source Cu, current was 30 mA, voltage was 40 kV, and the wavelength λ =1.5405 A^{o}.

2.7 D.C. Electrical Conductivity

To measure the DC conductivity of the prepared films, a system consisting of a DC power supply and a Keithley 8110G/8105G low-voltage current meter was used. A specific voltage difference was applied through the power supply, and the current passing through the film was read. By plotting the generated current with the applied voltage, the electrical resistance of the films was calculated as the reciprocal of the slope (1/Slop). Then, the electrical conductivity (σ) was calculated as one of the important electrical properties that determine the nature of the film's use.

2.8 Tensile

In this test, a tensile testing device of the type JIANQIAO TESTING EQUIPMENT was used, where the sample is fixed in the designated position between the jaws to hold the sample firmly and ensure that it does not move during the test. When the device is turned on, the handles begin to pull the sample from the top and bottom, with a value calculated through the device screen now of the sample's breaking (failure). Here, the tensile test was performed for each prepared polymer film, and its maximum tensile strength was determined.

2.9 Hardness

To calculate the hardness, a Shore-A hardness tester model TH200 was used. The Shore-A hardness tester model TH200, a hand-held device, consists of a spring-loaded needle-shaped insert that punctures the surface of the sample and then records the number that appears on the device's screen. Four readings were recorded at different locations, and the average was calculated.

3. RESULTS AND DISCUSSION

The morphology of the POT.TiO_2/PMMA, POT.TiO_2/PS, and POT.TiO_2/PEO films are shown in Figure 1. All images showed the coating of conductive and conventional polymers onto the TiO_2 nanoparticles, with smooth surfaces when blending with PMMA and PS. However, when coated with PEO, the surfaces of the TiO_2 nanoparticles became rough and disorganized. The TiO_2 nanoparticles in this polymer were well dispersed, leading to an increase in their diameter. Meanwhile, the POT/TiO_2

blend films showed a formation of interwoven structure and an enhancement in conductivity, similar to the results obtained by Haider et al. [13] and Adaikalam et al. [14]. FE-SEM images show that the morphology of POT.TiO_2/PMMA and POT.TiO_2/PS films is approximately similar; they appear as semi-spherical and spherical protrusions structures. The situation is different in POT.TiO_2/PEO, as morphology is rough and disorganized.

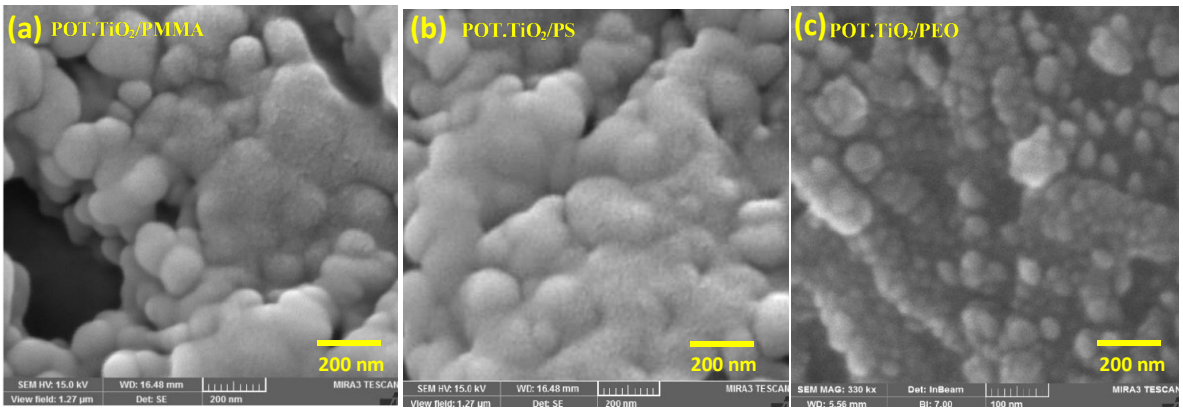

Figure 1: FE-SEM images of (a) POT.TiO_2/PMMA, (b) POT.TiO_2/PS and (c) POT.TiO_2/PEO films

Figure 2 displays the X-ray diffraction patterns of the POT.TiO_2 powder and POT.TiO_2/PMMA, POT.TiO_2/PS, and POT.TiO_2/PEO films. The X-ray diffraction pattern of POT.TiO_2 powder (Figure 2(a)) demonstrated characteristic peaks of polycrystalline POT.TiO_2 powder at 2θ = 25.44°, 27.4°, 37.68°, and 47.7°. The POT.TiO_2 powder also showed a crystalline peak at 2θ = 25.44°, with high intensity and sharpness. This peak, which is common in POT and TiO_2, denoted that long-range conjugation occurred. Due to the substantial improved conjugation in TiO_2 nanoparticles, this peak was substantially sharper in the POT.TiO_2 nanocomposite [7]. The peak in POT.TiO_2 X-ray diffraction pattern at 2θ = 47.7° disappeared, and it was offset by the growth of a new peak at 2θ = 15.16°. In the POT.TiO_2/PMMA and POT.TiO_2/PS films (Figures 2(b) and (c)), a strong peak around 2θ = 15.16° and peaks at 2θ = 25.44° and 27.4° were observed, which are the characteristic peaks of these blends [14]. The X-ray diffraction pattern of POT.TiO_2/PEO films shown in Figure 2(d) exhibited a growth of more peaks than in the two other films: strong characteristic peaks at 2θ = 22.9° and 26.2° and three peaks at 2θ = 15.16°, 25.44°, and 27.4°. Some peaks corresponded to the (120) reflection of the PEO structure at 2θ = 22.9°, other peaks corresponded to the PEO structure at 2θ = 25.44°, and the rest of the peaks indicated the structure of POT.TiO_2/PEO [15]. In all the films, the characteristic peaks indicated a polycrystalline structure. Meanwhile, the POT.TiO_2 powder showed low-intensity broad band peaks compared with the POT.TiO_2/PMMA, POT.TiO_2/PS, POT.TiO_2/PEO films, indicating that the addition of conventional polymers enhanced the crystallinity state of POT.TiO_2. Conventional polymers added to POT.TiO_2 powder that improve crystallinity by providing crystallization centers, limiting the movement of molecules, increasing contact between components, and forming separate phases this produces larger crystals and well-organized growth, appearing strong and sharp peaks in spectrum analysis.

The X-ray spectra can be used to compute the average crystallite size (C.S.) of the powder and films by using the full-width-at-half-maximum (FWHM) approach (Scherrer relation) as follows [16]:

$$C.S. = \frac{D\lambda}{\Delta\theta \cos\theta} \ldots\ldots\ldots \quad (1)$$

where Δθ is the FWHM of the XRD peak appearing at the diffraction angle θ; D is Scherrer's constant, usually assumed as D = 1; and λ is the X-ray wavelength. Table 2 shows the results of average C.S. The C.S. of the powder and films demonstrated approximately similar C.S. of 12.02 nm, except for the

POT.TiO_2/PEO film, which had a C.S. of about 27.56 nm, implying that this film had the best crystallization state.

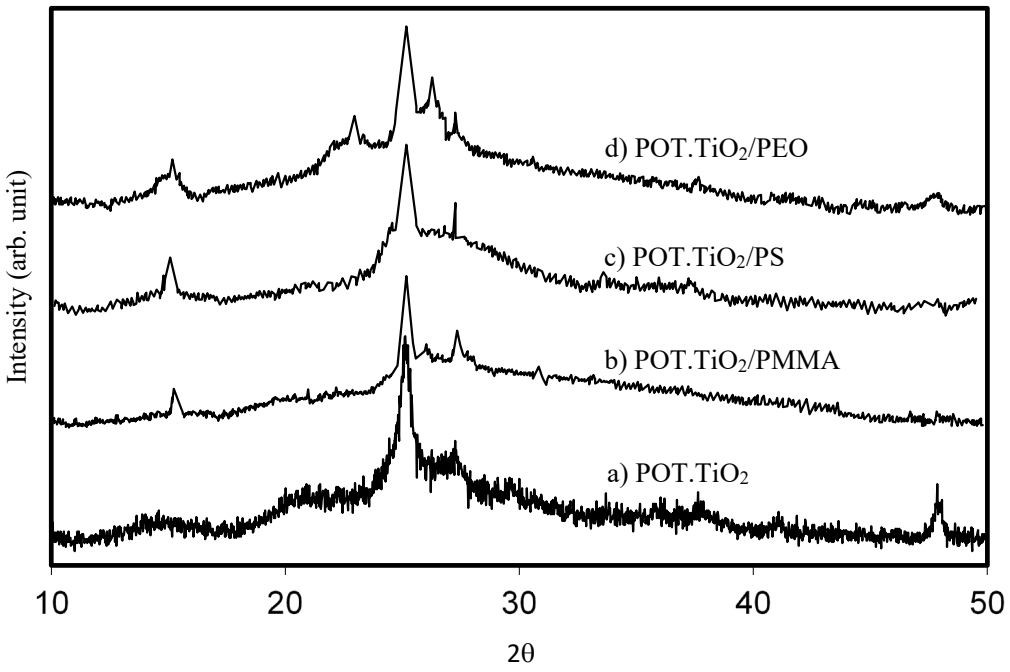

Figure 2: The XRD spectra of (a) POT.TiO_2 powder, (b) POT.TiO_2/PMMA, (c) POT.TiO_2/PS and (d) POT.TiO_2/PEO films.

Table 2: The physical parameters of POT.TiO_2 powder, POT.TiO_2/PMMA, POT.TiO_2/PS and POT.TiO_2/PEO films

Samples	Crystallite Size (C.S.) nm	Conductivity σ ($S.cm^{-1}$)	Tensile (MPa)	Hardness Shore A
POT.TiO_2 Powder	12.02	-----	-----	-----
POT.TiO_2/PMMA film	9.56	1.22×10^{-8}	7.98	112
POT.TiO_2/PS film	13.33	2.21×10^{-8}	6.76	118.5
POT.TiO_2/PEO film	27.56	2.81×10^{-8}	3.51	110.3

The FTIR spectra of POT.TiO_2 powder and POT.TiO_2 blends films are shown in Figure 3. The FTIR spectra of POT.TiO_2 powder (Figure 3(a)) showed a peak at 709 cm^{-1}, which was attributed to the Ti–O bonds. The peak at 911 cm^{-1} corresponded to the C–O–C vibration, and the peak at 1228 cm^{-1} corresponded to the conducting protonated state of POT. The presence of benzoid band around 1503 and 1596 cm^{-1} indicated the emeraldine salt form of POT in POT.TiO_2 nanocomposite. The band at 2998 cm^{-1} may be assigned to the C–H or C=C stretch bond. The strong and broad peak at 3314 cm^{-1} was attributed to the N-H stretching vibration of aromatic ring in POT. The peak at 3823 cm^{-1} represented the Ti–O–Ti and O–H stretching frequencies. Thus, the FTIR spectra confirmed the formation of POT-TiO_2 nanocomposites [17]. The FTIR spectra of POT.TiO_2/PMMA films are shown in Figure 3(b). The characteristic peaks at 733 and 3801 cm^{-1} were attributed to the TiO_2 bonds. The characteristic peak at 3454 cm^{-1} referred to the N–H stretching vibration in POT. The band around 2894–3022 cm^{-1} was attributed to C–H bond, and that at 1707 cm^{-1} may correspond to the C=O stretching in PMMA. The band at 1466 cm^{-1} represented the O–CH_3 deformation in PMMA, and the band at 1285 cm^{-1} referred to the C–N stretching mode of the benzenoid unit of POT [18].

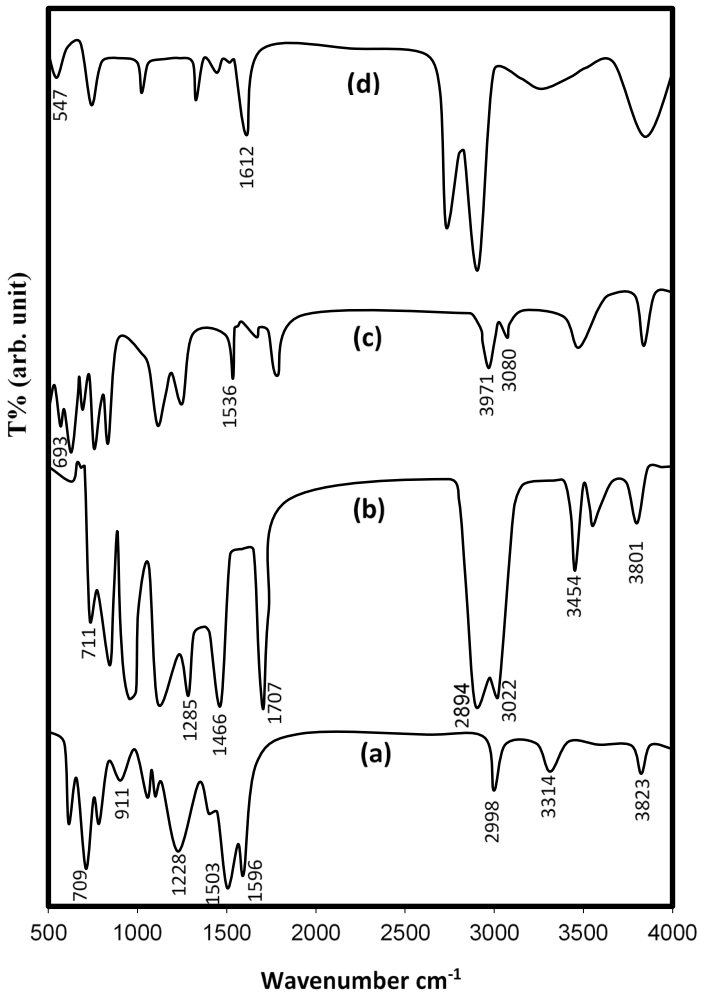

Figure 3: The FTIR spectra of (a) POT.TiO_2 powder, (b) POT.TiO_2/PMMA, (c) POT.TiO_2/PS and (d) POT.TiO_2/PEO films.

When mixing two polymers, their functional identity in the mixture has similar bond vibrations, leading to a change in intensity and sometimes shifting of the peak position due to the interaction between the nitrogen in POT/TiO_2 and the electron-deficient carbon center of PMMA [19]. The FTIR spectrum of POT.TiO_2/PS films shown in Figure 3(c) showed a peak at 3080 cm^{-1}, which may correspond to C–H aromatic stretching vibration. The peak at 2971 cm^{-1} was attributed to the asymmetrical and symmetrical stretching vibrations of CH_2. The stretching vibration of benzene ring can be attributed to the peak at 1536 cm^{-1}, and the peaks at 693 cm^{-1} were due to the C–H out-of-plane bending vibration of benzene ring. Moreover, some POT peaks overlapped with polystyrene peaks [20]. The FTIR spectrum for POT.TiO_2/PEO film is shown in Figure 3(d). Obvious changes were observed in the intensities, and a number of peaks were pronounced between 547 and 1612 cm^{-1} because of the significant interaction between the oxygen of the ether group of PEO and the nitrogen in the aniline of POT. The electrical characteristics of POT.TiO_2/PMMA, POT.TiO_2/PS, and POT.TiO_2/PEO films were examined. How changing the standard polymer may affect the electrical conductivity of films was explored. Studying the voltage–current characteristics is a necessary step in deciding the process of electrical conductivity in prepared samples. Figure 4 displays the current–voltage characteristics of the prepared films made with various standard polymers. The electrical conductivity values are listed in Table 2. The results revealed the maximum conductivity value of the POT.TiO_2/PEO film at about 2.81×10^{-8} S.cm^{-1} due to the enhancement in the structural properties of the film and the increase in crystallite size, which led to improved conductivity compared with the two other films. The increase in conductivity was also attributed to the good contact between POT.TiO_2 and the PEO quinoid rings [21].

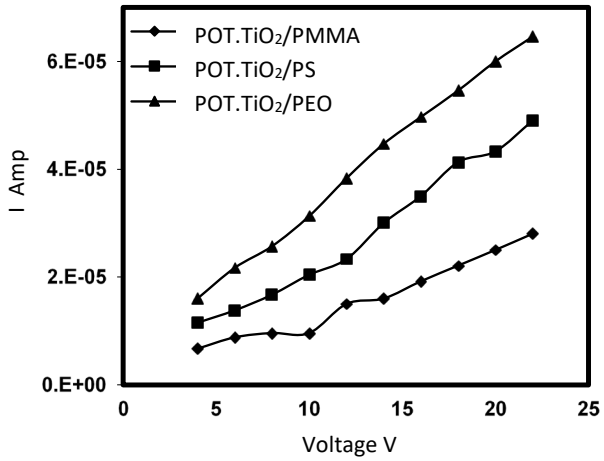

Figure 4: The (current-voltage) characteristic for POT.TiO_2/PMMA, POT.TiO_2/PS, POT.TiO_2/PEO films.

The mechanical properties were determined, mainly to investigate the effect of changing the conventional polymer on the tensile strength and shore A hardness behavior of POT.TiO_2 blends films. The tensile characteristics of POT.TiO_2 blends were altered by the interaction of conventional polymer molecules with POT.TiO_2. The tensile strengths of POT.TiO_2/PMMA, POT.TiO_2/PS, and POT.TiO_2.PEO films were measured, as shown in Table 2. The maximum tensile strength values of the POT.TiO_2/PMMA film were obviously higher than those of the two other films due to the high degree of miscibility between POT.TiO_2 and PMMA. Furthermore, the POT.TiO_2 dispersion in PMMA worked as crosslinking centers between the PMMA molecules by settling down at the voids and interface sites [4]. The resistance of a sample to localized plastic deformation, or, as it is known, the hardness, was measured for all samples. The micro hardness values of POT.TiO_2/PMMA, POT.TiO_2/PS, and POT.TiO_2/PEO films are shown in Table 2. The POT.TiO_2/PS film had higher hardness values of about 118.5 than the two other films, because the overlap and stacking restricted the mobility of the polymer molecules, thereby increasing the material's resistance to cuts, scratches, and plastic deformation [22]. Each sample has characteristics that make it suitable for a particular electronic application. POT.TiO_2/PMMA may be suitable for applications requiring insulation materials and complex devices such as capacitors and optical filters, while POT.TiO_2/PS is a suitable choice for applications such as transistors and insulating films on printed circuits. Finally, POT.TiO_2/PEO can use flexible devices like sensitive devices, batteries and wearable sensors.

4. CONCLUSIONS

The casting method was used to successfully prepare POT.TiO_2 blends films. The effects of different conventional polymers on morphology, crystallinity, functional groups, electrical conductivity, tensile strength, and shore A hardness of POT.TiO_2 blends films were investigated. The results showed well dispersed TiO_2 in the films. The XRD data exhibited the polycrystalline structure of all the films. According to the FTIR spectra, the modifications in conventional polymers with POT.TiO_2 resulted in the emergence of new peaks, clearly denoting the blend between POT.TiO_2 and conventional polymers. Lastly, the electrical and mechanical tests showed that the POT.TiO_2/PEO film had higher electrical conductivity and lower hardness and tensile values than the POT.TiO_2/PMMA and POT.TiO_2/PS films. This makes each sample it suitable for a particular electronic application.

Acknowledgments

The author would like to thank Mustansiriyah University (www.uomustansiriyah.edu.iq), Baghdad – Iraq for its support in the present work.

Author Contributions

All authors contributed toward data analysis, drafting, and critically revising the paper and agree to be accountable for all aspects of the work.

Disclosure of Conflict of Interest

The authors have no disclosures to declare

Compliance with Ethical Standards

The work is compliant with ethical standards

References

[1] Tadesse, M. G., Ahmmed, A. S. & Lübben, J. F. (2024). Review on conductive polymer composites for supercapacitor applications. *Journal of Composites Science*, 8(2), 53.

[2] Ding, H., Hussein, A. M., Ahmad, I., Latef, R., Abbas, J. K., Abd-Ali, A. T., Saeed, S. M., Abdulwahid, Al. S., Ramadan, M. F., Rasool, H. A. & Elawady, A. (2024). Conducting polymers in industry: A comprehensive review on the characterization, synthesis and application, *Alexandria Engineering Journal*, 88, 253-267.

[3] Abd El-Lateef, H. M. & Alnajjar, A. O. (2020). Enhanced the protection capacity of poly(o-toluidine) by synergism with zinc or lanthanum additives at C-steel/HCl interface: A combined DFT, molecular dynamic simulations and experimental methods. *Journal of Molecular Liquids*, 303, 253-267.

[4] Helyati, A-H. S., Ramli, M. M., Mohtar M. N., Rahman N. A. & Ahmad, A. (2021). Synthesis and conductivity studies of poly(methyl methacrylate) (PMMA) by co-polymerization and blending with polyaniline (pani). *Polymers,* 13(12), 1939.

[5] Jadaun, J. S., Bansal, S., Sonthalia, A., Rai., A. K. & Singh, S. P. (2022). Biodegradation of plastics for sustainable environment. *Bioresource Technology,* 347, 126697.

[6] Bandehali, S., Moghadassi, A., Parvizian, F., Hosseini, S. M., Matsuura, T. & Joudaki, E. (2020). Advances in high carbon dioxide separation performance of poly (ethylene oxide)-based membranes. *Journal of Energy Chemistry*, 46, 30-52.

[7] Aminuddin, N. F., Nawi, M. A. & Bahrudin N. N. (2022). Enhancing the optical properties of immobilized TiO_2/Polyaniline bilayer photocatalyst for methyl orange decolorization. *Reactive and Functional Polymers*, 174, 105248.

[8] Balan, R. & Gayathri, V. (2022). In-vitro and antibacterial activities of novel POT/TiO_2/PCL composites for tissue engineering and biomedical applications. *Polymer Bulletin*, 79, 4269–4286.

[9] Andrady, A. L. & Khan, S. A. (2022). *Applications of Polymer Nanofibers*. (John Wiley & Sons) pp. 130-139.

[10] Namsheer, K. & Rout, C. S. (2021). Conducting polymers: a comprehensive review on recent advances in synthesis, properties and applications. *RSC Advances*, 11(10), 5659-5697.

[11] Jameel, A. N. & Alwan, T. J. (2021). Effect of γ-ray irradiation on the physical properties of PANI/TiO_2 nanocomposite thin films. *Physics AUC*, 31, 6-13.

[12] Alwan, T. J. (2019). Effects of gamma irradiation on the physical properties of PANI.MWCNT/PMMA films. *Journal of Physical Studies*, 23(3), 3710.

[13] Haider, A. J., Al-Shibaany, Z., Hawy, R. & Hamed, N. (2020). Impact of PS/PMMA polymer ratios with nanocomposite material on optical and morphological properties. *Ziggurat Journal of Materials Technology*, 1(1), 23–32.

[14] Adaikalam, K., Vikraman, D., Lee, D-H., Cho, Y-A. & Kim, H-S. (2024). Optical and UV shielding properties of inorganic nanoparticles embedded in polymethyl methacrylate nanocomposite freestanding films. Polymers, 16(8),1048.

[15] Alsulami, Q. A. & Rajeh, A. (2022). Structural, thermal, optical characterizations of polyaniline/polymethyl methacrylate composite doped by titanium dioxide nanoparticles as an application in optoelectronic devices. *Optical Materials*, 123, 111820.

[16] Cullity, B. D. & Stock, S. R. (2011). *Elements of X-Ray Diffraction*. 3rd edition (Prentice Hall, Inc.) pp. 167-170.

[17] Balan, R. & Gayathri, V. (2022). In-vitro and antibacterial activities of novel POT/TiO_2/PCL composites for tissue engineering and biomedical applications. *Polymer Bulletin*, 79, 4269–4286.

[18] Aljarrah, I. A., Bani-Salameh, A. A., Ahmad, A., Al-Bataineh, Q. M., Ahmad, M. A., Al-Akhras, M-A. H. & Telfah, A. (2023). Effect of UV-illumination on refractive index of PMMA/Metal oxide nanocomposite films. *Polymer Bulletin*, 80, 7533–7543.

[19] Ramachandran, A. A., Reghunadhan, A., Maria, H. J. & Thomas, S. (2020). Role of functional polymers in the compatibilization of polymer blends. In *Reactive and Functional Polymers Volume Two*. Ed. Gutiérrez, T. J. (Springer Cham), pp. 5-21.

[20] Rahmouni, A. & Belbachir, M. (2014). New hybrid nanomaterial based on two polymers (pani and peo) in the interlayer galleries of an ecologic and friendly catalyst layered called maghnite-H+ (algerian MMT). *American Journal of Chemistry and Application*, 1(2), 34-39.

[21] Niaz, N. A., Shakoor, A., Hussain, F., Iqbal, M., Khalid, N. R., Saleem, M. K., Anwar, N. & Ahmad, J. (2022). Structural and electronic properties of PANI-ZnO-TiO_2 nanocomposite. *Journal of Ovonic Research,* 18(5), 713-722.

[22] Chen, A., Wang, T., Chen, Y., Wang, S. & Chen Y. (2022). Development of polystyrene/polyaniline/ceria (PS/PANI/CeO_2) multi-component abrasives for photochemical mechanical polishing/planarization applications. *Applied Surface Science*, 575, 151784.